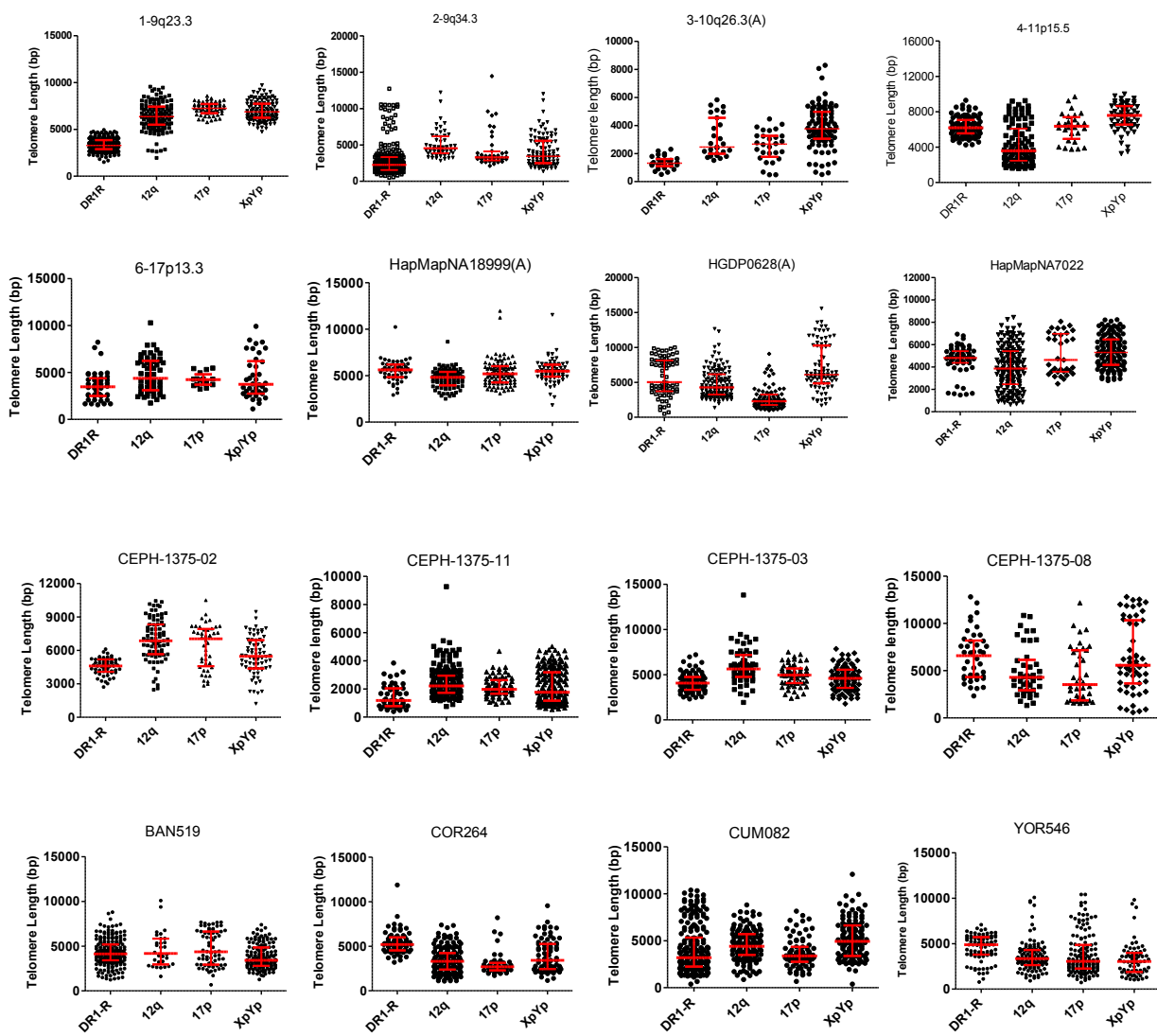
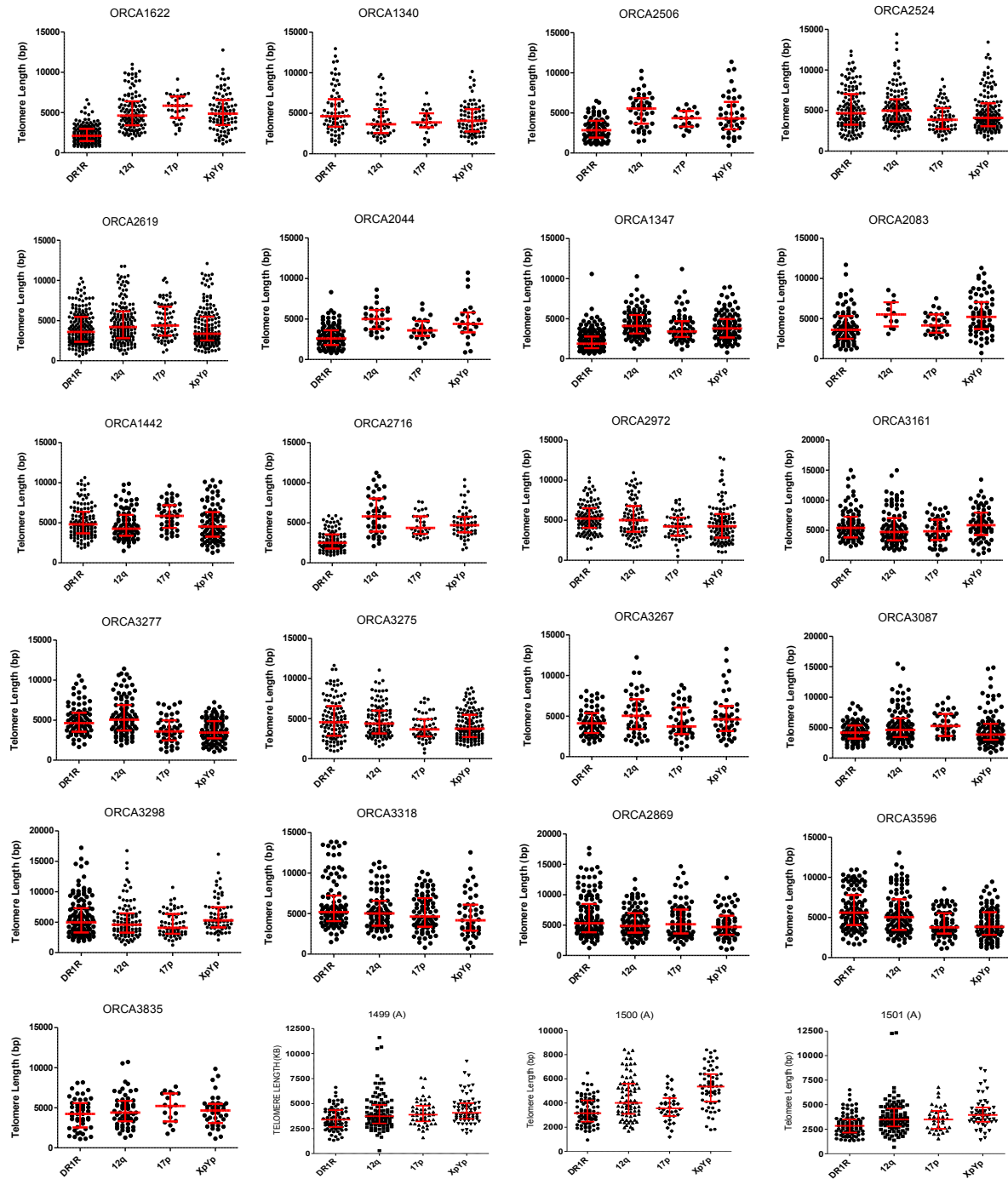


Supplementary Figure S2. Confirmation that the PAC1 sequence is present in DR_R but absent from the terminal DR_L in CI-HHV-6B carriers. (A) The diagram explains the assay used to detect the PAC1 sequence that contains a *SmaI* restriction site. (B) The PCR amplicon from the internal DR_R (generated with the DR1R and U100F2 primers) in four unrelated CI-HHV-6B carriers is shown undigested (Un-d); digested with *Sall* (positive control for digestion); digested with *SmaI* to detect the PAC1 sequence. These amplicons were cleaved by *SmaI* in all four donors showing that PAC1 is present in DR_R. STELA products were generated from DR_L in the four CI-HHV-6B carriers (1 to 3 amplicons per donor). The STELA products are shown undigested, digested with *Sall* or *SmaI*. All the amplicons are cleaved by *Sall* but none were cleaved by *SmaI* showing that the PAC1 sequence is missing from DR_L at the distal end of the integrated viral genome. The products were detected by Southern blot hybridization to a ³²P labeled (TTAGGG)_n probe.

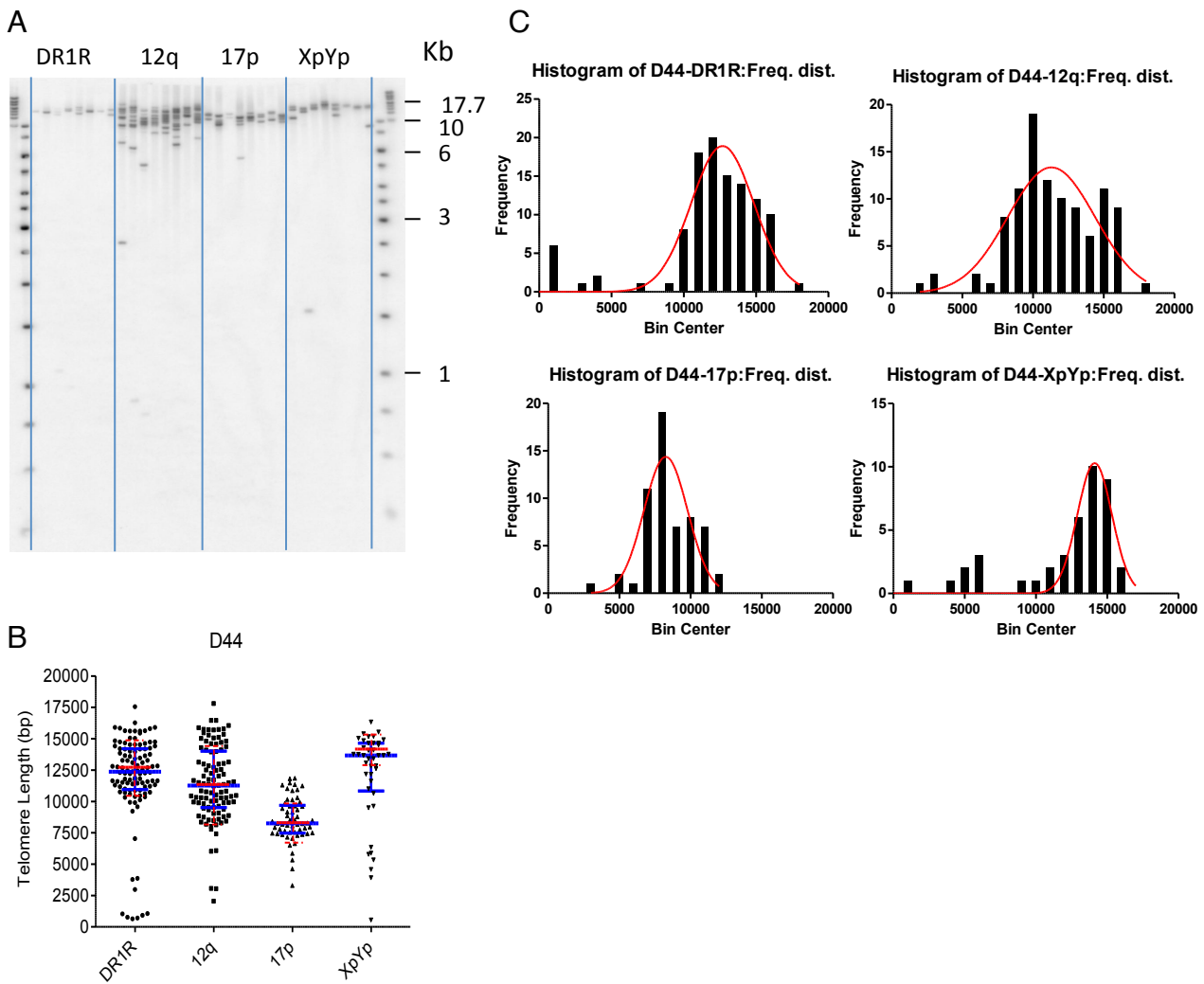


Supplementary Figure S3A (LCLs)



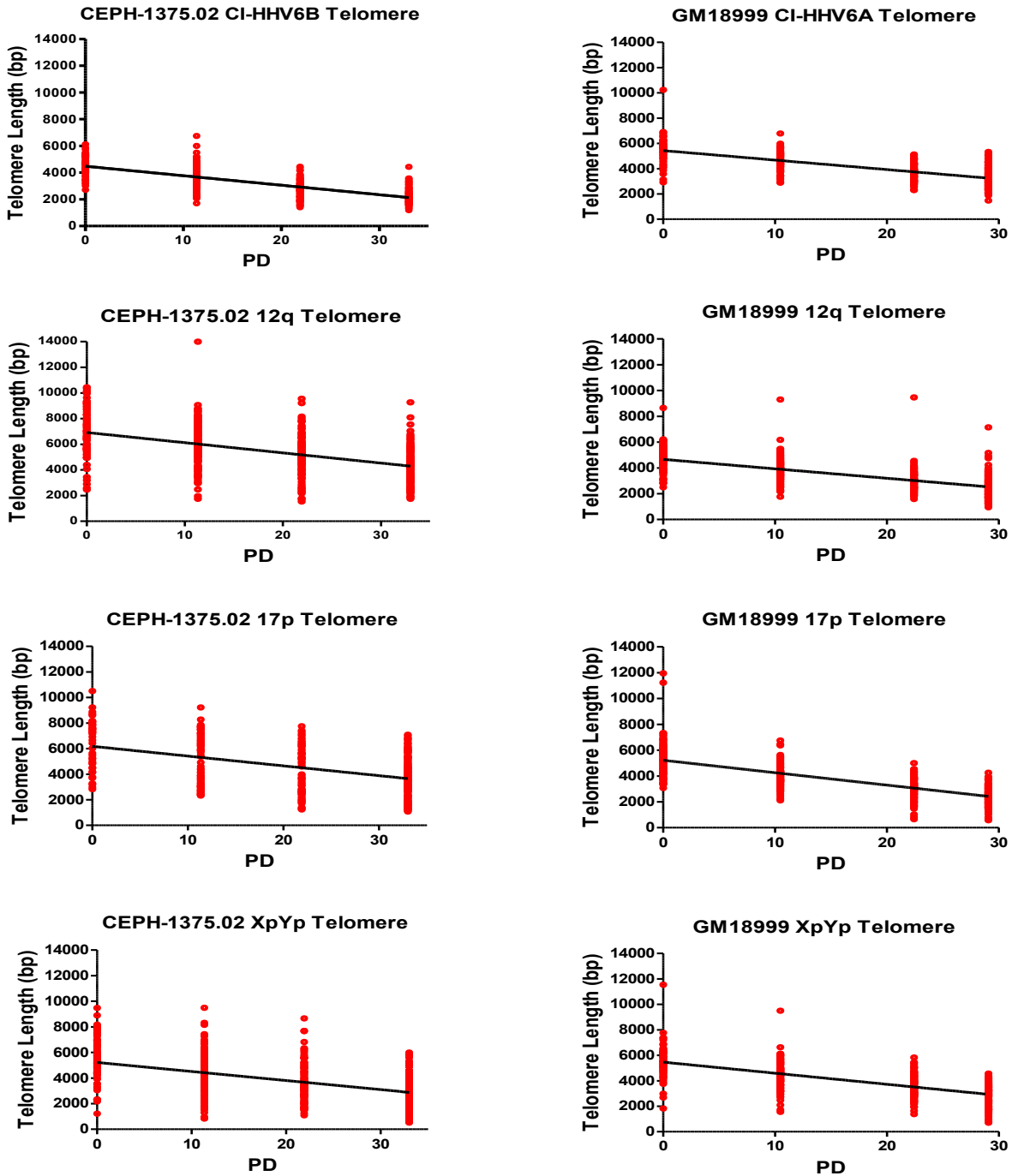
Supplementary Figure S3B (Blood DNAs)

Supplementary Figure S3. Comparative length analysis of the HHV-6 associated, 12q, 17p and XpYp telomeres in 40 CI-HHV-6A or B carriers. (A) The scatter plots derived from STELA length analysis at the four telomeres in 16 DNA samples derived from LCLs from CI-HHV-6 carriers. Samples 3-10q26.3, HapMapNA18999 and HGDP0628 are from CI-HHV-6A and the remainder from CI-HHV-6B carriers. **(B)** The scatter plots derived from STELA length analysis at the four telomeres in 24 DNA samples derived from blood from CI-HHV-6 carriers. Samples 1499, 1500 and 1501 are from CI-HHV-6A and the remainder from CI-HHV-6B carriers. The median value and inter-quartile range are shown as red lines.



Supplementary Figure S4. Telomere length analysis in sperm DNA. (A) A representative STELA blot used to measure telomere length in sperm DNA from donor 44 (D44). The blot shows amplicons from the CI-HHV-6-associated (DR1R), 12q, 17p and XpYp telomeres. (B) Summary scatter plots from the telomere length analysis in sperm DNA from D44. The median length and inter-quartile range are shown as blue lines and the mean from the best-fit normal distribution (shown in c) and standard deviation (SD) are shown as red lines. (C) The sperm telomere molecules were assigned to 1kb bins based on their length and the frequency of molecules in each bin plotted against length. A best-fit normal curve of the population of larger molecules was used to determine the mean length and SD.

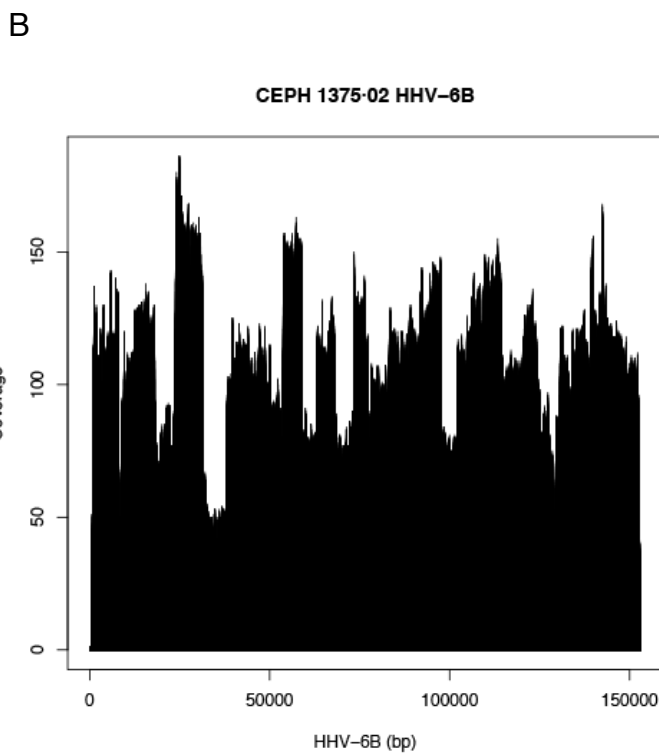
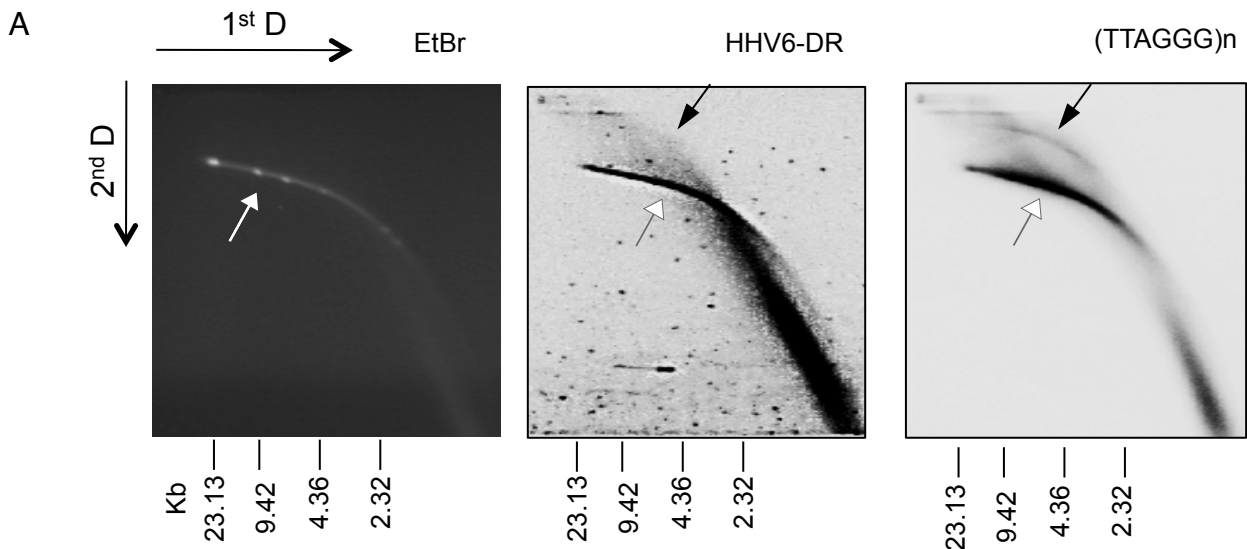
A



B

Telomere	Telomere shortening rates in CEPH1375.02 LCL	Telomere shortening rates in GM18999 LCL
CI-HHV6 telomere	71 ± 4	75 ± 5
12q telomere	80 ± 7	73 ± 4
17p telomere	77 ± 8	96 ± 4
XpYp telomere	71 ± 6	87 ± 5

Supplementary Figure S5. The rate of telomere shortening in LCLs from a CI-HHV-6A and a CI-HHV-6B carrier. (A) Telomere length (bp) plotted against increasing number of population doublings (PD) for the CI-HHV-6-associated, 12q, 17p and XpYp telomeres in the LCLs from CEPH1375.02 CI-HHV-6B and HapMapNA18999 CI-HHV-6A (GM18999). Linear regression analysis was used to produce a line of best-fit. **(B)** Table showing the telomere shortening rate (bp/PD) ± standard error at the four telomeres in each cell line.



Differences between HHV-6B HST and CI-HHV-6B in CEPH1375.02:

282 single base changes – none predicted to truncate ORFs
 Indels: 10 single base insertions; 2 x 2 base insertions; 1 x 3 base insertion
 6 single base deletions

None of the indels are predicted to cause frame-shifts. For example the U36 ORF includes 4 base substitutions, 2 x single base insertions and 2 x two base insertions (net gain 6 bases) relative to the HST strain. The predicted HHV-6B U36 amino acid sequence in CEPH1375.02 is 482aa and shows 99.8% identify to the Z29-HHV-6B U36aa sequence.

Homopolymer tracts: we found the IonTorrent sequence analysis was accurate up to A₁₀ or T₁₀ and up to C₆ or G₆. Therefore for polyA/T tracts >9 and polyC/G >5 we assumed the sequence in 1375-CI-HHV-6B was the same as the reference sequence HST.

Two segments, over the repetitive R3 region and the U1 region are currently unfinished.

Supplementary Figure S6. Extra-chromosomal circular DNA containing DR sequences and summary of sequence analysis from CI-HHV-6B in CEPH1375.02 (A) Two-dimensional agarose gel electrophoresis of genomic DNA from CEPH1375.02 CI-HHV-6B following digestion with *Eco*RI and Plasmid-safe DNase. The panel on the left shows the migration of the linear DNA size marker (sizes shown below); the middle panel shows the 2D gel following Southern blot hybridization to detect HHV-6 DR sequences; the right panel shows the same Southern blot hybridized to the telomere probe. The black arrows shows the arc of the relaxed circular molecules containing DR sequences (middle panel) or (TTAGGG)_n (right panel; these could be derived from all telomeres and are more abundant than the DR containing circles). The white arrows show the migration of residual linear DNA (co-incident with the size marker). (B) Diagram showing next-generation sequence coverage of the CI-HHV-6B genome from CEPH1375.02. The short reads generated by IonTorrent sequencing (total = 194,439) included duplicates that were identified and removed using Picard (Sourceforge). Following identification and removal of duplicate reads the plot of coverage (number of reads per base) of the remaining 120,117 reads across DR_L and the unique region was generated using Bedtools. The differences between the CI-HHV-6B in CEPH1375.02 and the HST strain are summarized.